UNIVERSITÀ DEGLI STUDI DI PADOVA

DIPARTIMENTO DI BIOLOGIA

Corso di Laurea magistrale in Biologia Sanitaria

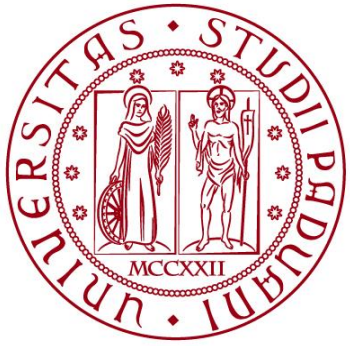

TESI DI LAUREA

YAP1 DEPENDENT REGULATION OF MITOCHONDRIAL DYNAMICS IN ADIPOCYTES

Relatore: Prof. Luca Scorrano
Dipartimento di Biologia

Correlatore: Camilla Bean
Istituto Veneto di Medicina Molecolare

Laureanda: Ludovica Zambello

ANNO ACCADEMICO 2021/2022

CONTENTS

1. ABSTRACT

The unique characteristic of the adipose tissue relies in its plasticity: the adipocytes can adapt their structure, size and metabolism to accommodate more lipids, thus protecting the body from lipotoxic events and contribute to the whole-body homeostasis. Disruptions in this adaptability results in pathological conditions, such as lipoatrophy. Preliminary data suggested that the mitochondrial shaping protein OPA1 plays a key role in the size modulation of adipocytes with a predicted involvement of the HIPPO pathway and its effector YAP1. To assess the possible interplay between YAP1 and OPA1 in the physiology of the adipocytes, we used a $OPA1^{\Delta AT}$ murine model characterized by spontaneous lipoatrophy. We challenged our model with 4 weeks of HFD to impinge in the adipose response hypertrophy and hyperplasia responses. Combing western blot analysis, qRT-PCR technique and immunofluorescence, we identified a downregulation of YAP1 and its effectors genes in whole subcutaneous tissue of $OPA1^{\Delta AT}$, which corresponded to a lower translocation of YAP1 in the nuclei of KO mature adipocytes. In vitro models further confirmed an alteration of YAP1 total amount when OPA1 is knock out through Adenocre transfection. Interstingly, qRT-PCR analysis of YAP1 main target suggested a more complicate scenario with the possible involvement of YAP1 paralog, TAZ.

2. INTRODUCTION

2.1 The adipose tissue: role and physiology

The adipose tissue is an organ specialized in the synthesis, mobilization and storage of fat. Far from being a simply passive reservoir of energy, this organ is deeply implicated in the maintenance of the whole-body homeostasis and metabolism[1,2].

We can identify two main types of fat deposit, named the white adipose tissue (WAT) and the brown adipose tissue (BAT), which differentiate for their functions, morphological feature and localization[3].

The white adipose tissue is characterized by cells with a single large lipid droplet, which occupies most of the cytoplasmatic space so that the nucleus and mitochondria are confined against the plasma membrane. It plays key physiological functions in energy storage, insulin sensitivity and endocrine communication [2]. Indeed, this deport secrete a variety of peptide hormones called adipocytokine (such as leptin, adiponectin, resistin) which play a critical role in regulation of food intake, energy expenditure, fuel metabolism and inflammatory response. Anatomically, this tissue comprises two major depots: a subcutaneous (SAT) and a visceral (VAT) one. The former is localized in beneath the skin, while the latter can be found in the abdominal cavity[11].

The brown adipose tissue is characterized by smaller multilocular cells and is involved in non-shivering (or adaptive) thermogenesis, thanks to the high concentration of mitochondria expressing the uncoupling protein 1 (UCP1)[4]. This protein dissipates energy in the form of heat by uncoupling the mitochondrial proton gradient, with no final production of ATP [4,5].

Recently, it has been identified a third type of fat deport, named “brite” or “beige” adipose tissue. It consists in a cluster of cells with similar morphologic features to classical brown adipocytes (central nuclei, multilocular lipid droplets, and are rich in mitochondria) without distinctive anatomical localization[6]. These cells are UCP^{+}, but present a lower basal level if compared with the BAT cells. Nevertheless, they are capable of a complete thermogenic switch, under exposed to β- adrenergic or

cold stimuli[1]. These intermediate cells gained a lot of interest for their potentiality in the treatment of obesity[5].

2.2 Adipose tissue dysfunction: from obesity to lipoatrophy

Obesity is defined by the World Health Organization (WHO) as the abnormal or excessive fat accumulation that represent a threat for the health. Indeed, this condition is associated with the leading causes of death, such as diabetes, heart disease, stroke, and some types of cancer[7].

Given the current world obesity epidemic, great effort has been done in the past decades to understand the molecular mechanism underlying the physiology of the adipose tissue and its disruption in the onset of pathological condition. When a subject is exposed to high caloric diet, the white adipose tissue responds enhancing its size, both in terms of cell dimensions (hyperthrophy) and cell number (hyperplasia)[3]. Thanks to this incredible adaptability, the adipose tissue is able to safely store the caloric excess in form of neutral lipids, thus protecting the organism from lipotoxic phenomena[8]. Nevertheless, this ability of the adipose tissue is limited, and once the cell has reached exhaustion, it undergoes an apoptotic cell death[9]. This is followed by macrophagic infiltration as a physiological event required for the clearance of the dead cell [10]. This process, if prolonged in time, cause a low-grade chronic inflammation which a crucial risk factor for the development of insulin resistance and type 2 diabetes in obese individuals[11]. Molecular mechanisms underlying this switch from a “healthy” to an “unhealthy” expansion are not so clear: possibly the total adipose tissue in an individual may have a maximal fixed capacity for safely storing fat. This could be determined by multiple factors like a finite number of pre-adipocytes, genetic programming of adipogenesis, vasculogenesis or functionality of other cellular components within the adipose tissue[9].

Lipoatrophy is the opposite event to obesity; it a condition that involve the loss of fat mass, in particular subcutaneous adipose tissue, in the absence of malnutrition or a catabolic state that would otherwise explain the fat loss[12]. Understanding the

molecular mechanism underlying this phenomenon could help in the further advancing in the treatment of obesity.

2.3 The role of mitochondrial dynamics in the white adipose tissue

Multiples studies have found that mitochondrial function is a main determinant of adipose tissue activity both in lipid mobilization and storing[13]. Recently, it has been reported in Bean et al., that OPA1 overexpression in the adipose tissue favors adipocyte plasticity, resulting in overall improved glucose metabolism and insulin sensitivity[5]. In particular, Opa^{tg} adipocytes are smaller when feed with standard diet, but can expand to a greater size than control WT adipocytes upon high fat diet (HFD) challenge. Vice versa, it was reported that mice lacking OPA1 selectively in the mature adipocytes displayed a lipoatrophic phenotype, with impairment in the metabolic activity.

Mitochondria play a central role in energy conversion and they are involved in a variety of processes[14]. In the white adipocytes, mitochondria regulate the balance of lipogenesis and lipolysis. Through cyclic event of fusion and fission, they allow lipid mobilization. [13] The dynamic morphology of the mitochondria is dictating by a group of protein, named dynamin: cytoplasmic GTPase Dynamin-related protein 1 (Drp1) plays a key role in mitochondrial fission with mitochondrial Fission protein 1 (FIS1) while Mitofusin1 (Mfn1), Mitofusin 2 (Mfn2) and OPA1 are involved in mitochondrial fusion[15].

2.4 YAP1 and its role in the adipose tissue

Yes associated protein 1 (from now on YAP1) is a key transcriptional factor of the HIPPO pathway. This signaling pathway is primarily involved in the regulation of stem cell self-renewal, organ size and tissue regeneration by regulating cell proliferation, differentiation and apoptosis[16]. This pathway is comprised of a cascade of intracellular kinases that ultimately phosphorylate and inhibit the downstream transcriptional regulators YAP1 (Yes-associated protein 1) and TAZ

(or WWTR1, WW domain containing transcription regulator 1) causing their sequestration and degradation in the cytoplasm. When dephosphorylated, thus activated, YAP1/TAZ migrates to the nucleus where they act as transcriptional co-activator or co-repressor by stabilizing different transcription factors, especially the TEA domain family members (TEAD)[17].

The implications of YAP/TAZ in the adipose cell have been extensively reported, nevertheless remaining still poorly characterized. For instance, the expression of PPARγ2, the master regulator of adipogenesis, is negatively regulated by the activation of TAZ in a HIPPO dependent manner[18]. Indeed, it has been reported that also the downregulation of YAP1 is required for adipogenic commitment[19]. Controversially, the activation of YAP1 and TAZ is required to protect the mature adipocytes from apoptotic events during High feed diet challenge[20].

Much still needs to be undercover about the role of YAP1 in the adipose tissue, making it a compelling subject of study.

2.5 Yap1 and the mitochondrial dynamics

Mitochondria play a central role in energy conversion and they are involved in a variety of cellular processes[14]. Besides their functional versatility, they are characterized by a dynamic morphology, as they continuously and reversibly rearrange their structure through continuous event of fusion and fission. In these dynamical changes cytoplasmic GTPase Dynamin-related protein 1 (Drp1) plays a key role in mitochondrial fission with mitochondrial Fission protein 1 (FIS1) while Mitofusin1 (Mfn1), Mitofusin 2 (Mfn2) and OPA1 are involved in mitochondrial fusion[15].

The processes regulated by YAP1 and TAZ (such as cell growth and proliferation) are generally high energy consuming. To support such a high demand, the cell is required to undergo a metabolic reprogramming, thus evidencing the central role of mitochondrial function[21]. YAP1 has been shown to pilot mitochondrial dynamics. For instance, YAP1 dependent increase of Drp1, and Mitofusion 2 (Mfn2) is crucial for the activation of myoblast differentiation[22].

Notably, preliminary observation in our lab, confirmed that the KO of YAP1 in the adipose tissue correlated with a high amount of OPA1, in the BAT deport, thus suggesting a possible interplay between these two proteins.

3. AIM OF THE THESIS

Recently it was observed that the inner mitochondria protein OPA1 is able to modulate the size of the adipose tissue, thus affecting the survival, function and metabolism of the adipocytes. Strong evidences suggest that YAP1 plays a key role in this process. With this thesis we aimed to investigate the possible interplay between OPA1, the mitochondrial dynamics and the YAP1 pathway. To achieve so we used both in vivo and in vitro models of mice $Opa1^{\Delta AT}$ focusing on modulation of YAP1.

4. MATHERIAL AND METHODS

4.1 Animal care and handling

Animals were housed in an animal facility on a 12h light/dark cycle at the room temperature of 22–24°C with free access to standard food and water, if otherwise stated, with no more than six animals accommodated per cage. To generate constitutive adipose- specific Opal knockout mice ($Opa^{\Delta AT}$), $Opa^{f/f}$ animals were crossed with transgenic mice expressing Cre under the control of the Adiponectin promoter (Adipoq-Cre, JAX #010803). $Opa^{f/f}$ /Cre^{-} littermates were used as controls. PCR genotyping was performed with the following primers (Table 1):

Opa	Forward	CAGTGTTGATGACAGCTCAG
	Reverse	CATCACACACTAGCTTACATTTGC
Cre	Forward	GGATGTGCCATGTGAGTCTG
	Reverse	ACGGACAGAAGCATTTTCCA

Table1: Primers used for genotyping.

using Mytaq extract-PCR kit (Bioline). Briefly, 20 µl of Buffer A, 10 µl of Buffer B and 70 µl of water DNAsi/RNasi free were added to each sample. Denaturation was performed as so: 75°C in agitation for 10 minutes, followed by 95°C for other 10 minutes and lastly in ice to stop the process. PCR was then performed in a 10 µl volume using the following mix: my Taq red 5 µl, H_20 2.8 µl, primer forward 0.6 µl (10 µM), primer reverse 0.6 µl (10 µM), sample 1 µl. PCR program: 94°C 4 min, for 40 cycles 94°C 40 sec, 56°C 40 sec, 72°C 40 sec, finally 5 min 72°C. Samples were run in a 2% Agarose gel.

4.2 In vivo treatment

Mice were fed with a HFD (Rodent Diet with 60% kcal% fat, Research Diets, Inc. D12492) for 4 weeks, starting at the age of 16 weeks. Weight and body composition were measured weekly using nuclear MRI (EchoMRI-100H Body Composition Analyzer, EchoMRI LLC).

For Glucose tolerance test (GTT) mice were fasted overnight before the start of the experiment. In the morning basal blood glucose was sampled, then mice were administrated, by intraperitoneal injection, with a dose of 2 mg kg−1. Blood samples were collected at the indicated time points from tail blood using a glucometer (FreeStyle).

For Insulin sensitivity test (ITT) mice were fasted for 5 hours before the start of the experiment, basal blood glucose was sampled and then mice were administrated intraperitoneally with 1 unit per kg of insulin (Humulin R 100UI/ML, Eli Lilly and Company). Blood glucose was analyzed at the indicated time intervals from tail blood using a glucometer (FreeStyle).

4.3 Mouse primary adipocytes

Adipose tissue was collected in DMEM/F12 (GIBCO, Invitrogen) added with antibiotics Penicillin and Streptomycin (1:50). All following steps were performed under sterile working condition, all the used solutions were freshly prepared and filtered using 0.22 µm sterile filter (Merck Millex GP syringe filter unit). The tissue was chopped using sterile scissor, necrotic tissue, vessels and fibers were removed. Digestion was performed with a sterile collagenase type II solution (0.5 mg/ml Sigma-Aldrich) with DMEM/F12 and glutamine (1:100) for 40 minutes at 37°C hot tub in agitation. After this, the medium was pipetted well with p5 ml to shred the remaining tissue and centrifuged at 322 g for 10 minutes at room temperature. The supernatant was eliminated by inversion and the pellet was resuspended in 5 ml of sterile DMEM/F12 FBS 3% supplemented with Glutamine and PenStrep (1:100). The first filtration occurred using a sterile steel strainer to

get rid of bigger collagen fibers, 5 ml of DMEM/F12 FBS 3% was added directly to the filter. After another centrifugation at 322 g for 8 minutes, the pellet was resuspended in 5 ml of sterile Lysis buffer (NH4Cl 1.545 M, KHCO3 100 mM, EDTA 1.27 mM) for 5 minutes to eliminate the red blood cells. Lysis was blocked adding 10 ml of sterile of DMEM/F12 FBS 3%, and the whole medium was then transferred in a new Falcon tube using 100 µm Easy strainer filters (Falcon). 8 minutes centrifuge at 322 g, pellet was resuspended in an adequate volume of sterile DMEM/F12 FBS 10%. Cells were then counted using a NEUBAUER chamber and seeded in an adequate volume of DMEM/F12 supplemented with 150 U/ml streptomycin, 200 U/ml penicillin, 2 mM glutamine, 1 mM HEPES (GIBCO, Invitrogen) and 10% FBS following the present scheme (Table 2):

Type of plate	**Cell number**	**Medium**
6 wells	2-2.5*10^6	2-2.5 ml
12 wells	1-1.5*10^6	600 µl-2 ml
24 wells	350-500*10^3	400 µl-1.5 ml
48 wells	100-250*10^3	300 µl-1 ml

Table2: Number of cells seeded for each type of plate. Medium amount is indicated.

Plates were then incubated at 37°C, 5% CO_2, to allow the cells to attach. At confluency, and anyway no more that 24 hours after seeding, the medium was replaced with Adipogenic Medium (MAD) containing 66 nM insulin, 100 nM dexamethasone, 1 nM T3, 0.25 mM IBMX, 10 µM rosiglitazone in standard medium 5% FBS to induce adipocytes differentiation. IBMX and rosiglitazone were removed after 3 days of culture. Cells were harvest until day seven when they reached complete maturation.

4.4 Cell transfection

GFP and AdenoCre viruses were gently gifted by our colleague Martina Semenzato.

Briefly, after extraction cells were seeded at the desired number in DMEM/F12 supplemented with 2 mM glutamine, 1 mM HEPES (GIBCO, Invitrogen) and 5% FBS, Adenovirus was directly added to the well at a concentration of 10 µl per ml of media. Cells were housed at 37°C, 5% CO_2, every 15 min for the first hour the plate was stirred by gently shaking. After 24 hours, the media was discharged, and cells were supplemented with MAD containing IBMX and rosiglitazone to induce differentiation. Efficiency of the transfection was assessed by western blot.

4.5 Western blot

Protein lysates was obtained either from snap-frozen tissues or cells and lysed in RIPA buffer: 50 mM TrisHCl, 1 mM EDTA, 150 mM NaCl, 1% NP40, 0,5% Sodium deoxycholate, 0,1% SDS supplemented with protease and phosphatase inhibitor cocktails, one tablet/10 ml buffer (Sigma). Protein lysates were clarified to eliminate the high lipid content by sequential centrifugation steps (4 °C, 20 min, 12,000g). Protein concentration was determined using Pierce BCA Protein Assay Kit (ThermoFisher 23225). An equal amount of protein was loaded and supplemented with gel sample buffer (Invitrogen) and 1 mM dithiothreitol. Samples were then boiled for 15 min at 95°C, separated on gels (Expressplus, Genscript), and transferred to polyvinylidene difluoride (PVDF) membranes (Immobilon P, Millipore). Membranes were then probed with the following antibodies as indicated in the figure legends: anti-OPA1 (1:1000 overnight, BD Biosciences 612607); anti-YAP1 (1:1000 overnight NovusBio NB110-58358); anti-Phospho-YAP (Ser127) (1:1000 Cell signaling 4911); anti-TAZ (1:1000 overnight, Santa Cruz Biotechnology 518026) ; anti-DRP1 (1:1000 overnight, ABclonal A2586), anti-Mfn2 (1:1000 overnight, Santa Cruz Biotechnology 515647), anti-Vinculin (1:7000 2 hours RT, V9264 Merk), anti-OXPHOS cocktail (1:1000 overnight, Abcam MS603-300).

Secondary isotype-matched antibody incubation conjugated to horseradish peroxidase followed for 1 hour at room temperature and signal detection was detected with ECL (Invitrogen) in ImageQuant LAS 4000.

4.6 RNA isolation and Gene Expression analysis

Total RNA was purified either from primary cells using the RNeasy Mini Kit (Qiagen) following producer instruction or from whole tissue lysate using Trizol (Invitrogen 15596-018). RNA was quantified by spectrophotometry using Nanodrop One (ThermoFisher), the purity was assessed by the absorbance ratios of 260:280 and 260:230 nm. Complementary DNA was generated with GoScript Reverse Transcription Mix (Promega) using an equal amount of RNA for each sample. The procedure is the following: the sample was first added with 1 µl oligodT and 1 µl dNTP, then denatured for 5 minutes at 70°C. Subsequently each sample was added with 5,7 µl of second mix (4 µl Buffer 5X, 1,2 µl $MgCl_2$, 0.5 µl Superscript). RtPCR was then performed with the following method: 25°C for 5 minutes, 42°C for 60 minutes, 70°C for 15 minutes. Triplicates 10 ng cDNA samples were then amplified using GoTaq qPCR Master Mix kit containing SYBR green fluorescent dye (Promega) in the QuantStudio 5 Real- Time PCR System (Thermo Fisher). The designed primers sequences are shown in Table 3. Actin was used as housekeeping gene as internal control for cDNA quantification and normalization, if otherwise stated. Relative changes in gene expression were determined by the $2^{(-\Delta\Delta C(T))}$ method.

Target	Sequence	
Opa1	Forward	ATACTGGGATCTGCTGTTGG
	Reverse	AAGTCAGGCACAATCCACTT
Yap1	Forward	CCTTTGAGATCCCTGATGATG
	Reverse	TCCTGCCATGTTGTTGTCTG
Lats1	Forward	GACTGGTGGAGTGTTGGTG
	Reverse	CAGAGGCTTCAGGACTCAGC
Lats2	Forward	GCGTCGGTGTGATTCTCTTT
	Reverse	AGCTTCGTGATGAGGTCTCG
Amotl2	Forward	AGACAACACCTCTGCCTGCT
	Reverse	CACTGCCTCCTTCCTTCAGA

CTGF	Forward	CCTGGTCCAGACCACAGAGT
	Reverse	TTTTCCTCCAGGTCAGCTTC
Cyr61	Forward	GAAATGCATCGTTCAGACCA
	Reverse	CTGCATTTCTTGCCCTTTTT
Pparγ2	Forward	TTCGTCGATGCACTGCCTATGA
	Reverse	GAATGCGAGTGGTCTTCCATCA
Actin	Forward	ACGGCCAGGTCATCACTATTG
	Reverse	AGGAAGGCTGGAAAAGAGCC
Pref1	Forward	ATGTCTGCAGGTGCCATGTT
	Reverse	CAAGTTCCATTGTTGGCGCA

Table3: Primers used for qRT- PCR.

4.7 Histology and immunofluorescence

Adipose tissue samples were fixed overnight at 4 °C in 4% paraformaldehyde (PFA) and then dehydrated through serial ethanol concentrations for paraffin embedding. Mayer's hematoxylin and eosin (H&E) was performed. For immunofluorescence staining paraffin-embedded sections of SAT were deparaffinized with xylene and rehydrated. Antigen retrieval was performed with heat in citrate buffer pH 6 (1,47 g of Sodim Citrate in 500 ml of ddH20, pH adjusted to 6 and then 2,5 ml Tween 10% was added). Blocking was performed with Goat Serum 10% (Sigma G9023). Sections were incubated with 1:200 anti-YAP1 (Santa Cruz SC101199) and 1:400 anti-TOM20 (Protein tech 11802-1-AP) overnight at 4 °C in humid chamber. Next day Donkey anti-mouse IgG Secondary antibody Alexa Fluor 488 (ThermoFisher A-21202; 1:200) and Goat anti-rabbit IgG Alexa Fluor 568 (ThermoFisher A-11011, 1:200) for 2h at rt in dark humid chamber. Nuclei were counterstained with 4.6-diamidino-2-phenylindole (DAPI) (Merck F6057). Finally, samples were treated with TrueVIEW Autofluorescence quenching kit (Vector SP-8500) according to manufacturer recommendation. Images were aquired using Zeiss Airyscan LSM 900. Analysis of adipocytes size was performed on H&E-stained 8-µm-thick sections using ImageJ.

4.8 Pure mitochondria extraction

Pure mitochondria were extracted from whole subcutaneous adipose tissue, freshly extracted. All following procedures were performed in ice, all used buffers were ice-cold. Briefly, under sterile condition the tissue was washed several times in Isolation Buffer (IB, 200mM Sucrose, 10 mM Tris-MOPS, 1mM EGTA-Tris pH 7.4 adjusted with Tris-Base 1 M at 4°C) and then minced into small pieces in 1 ml of IB. Shredded tissue was transferred in 2ml glass potter, 1 ml of IB was added and homogenization was performed using a Teflon pestle operated at 1600 r.p.m. (10 times, twice). Homogenate was centrifuged at 600 g, 4°C for 10 min, supernatant was collected and transferred to a clean Eppendorf to be centrifuged at 7000 g, 10 min at 4°C. Supernatant was collected as cytoplasmatic fraction and supplemented with protease inhibitors (PIC, Sigma). Mitochondria pure pellet was resuspended in IB and transferred to a new Eppendorf to be centrifuged at 7000 g, 10 min at 4°C (washing step). The resulting clean pellet was resuspended in RIPA buffer supplemented with protease and phosphatase inhibitor cocktails, one tablet/10 ml buffer (Sigma). Protein concentration was determined using Pierce BCA Protein Assay Kit (ThermoFisher 23225).

5. RESULTS

5.1 Mice Opa1 $^{\Delta AT}$ undergo progressive lipoatrophy since early age

Lipoatrophy is the condition for which the health of the adipose tissue is altered, and the subject experience pathological loss of fat mass in one or more adipose depots. Because the adipose tissue plays a pivotal role in the maintenance of the whole-body homeostasis, its disruption results in the onset of metabolic conditions such as insulin resistance, glucose intolerance and arise of lipotoxic phenomena.

As recently described in Bean et al., 2021, the adipose tissue specific deletion of OPA1 in mice (from now on Opa1$^{\Delta AT}$) causes a strong lipoatrophic phenotype, affecting all the adipose depots . Three months old Opa1 $^{\Delta AT}$ mice, show loss of fat mass, fibrotic deposition and impaired metabolic functions. With ageing Opa1 ΔAT mice lost completely the fat mass. However the food intake is comparable in young Opa1$^{\Delta AT}$ mice while even significantly increased in old Opa1$^{\Delta AT}$ mice compared to control littermates.

To understand the underlying causes of the observed lipodystrophy we decided to investigate the onset of adipose tissue loss in Opa1 $^{\Delta AT}$ mice.

During the first weeks of life WAT undergoes a strong white to beige remodelling, to support the thermogenic needs of the animal [23]. Beige adipocytes display a radically different biology and functions compared to white adipose tissue, because of its mainly implication in adaptive thermogenesis [1]. In order to avoid possible confusion in the study of the white adipose tissue, we decided to evaluate mice as young as 2 months old, when the WAT deport reached complete maturation[24]. Results are showed in Figure 1 and 2.

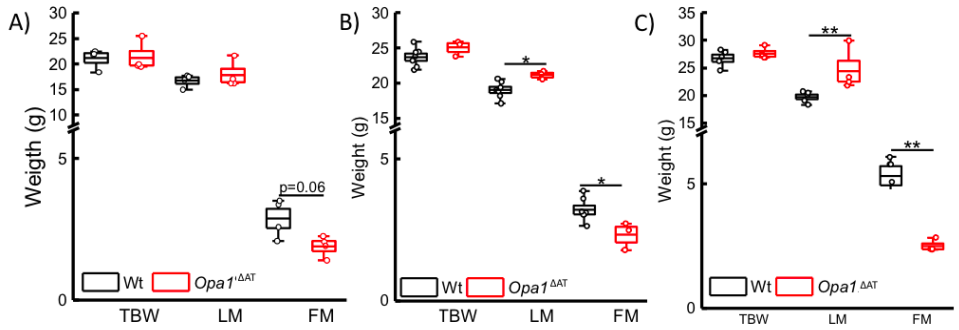

*Figure 1. Boxplot for total weight, fat mass and lean mass of WT and OPA1 KO mice at the age 8 (A), 12 (B) and 18 (C) weeks old, measure acquired by ECHOMRI technology. N>3 for each genotype and age. ** p<0.01, * p<0.05 in a two tailed Ttest.*

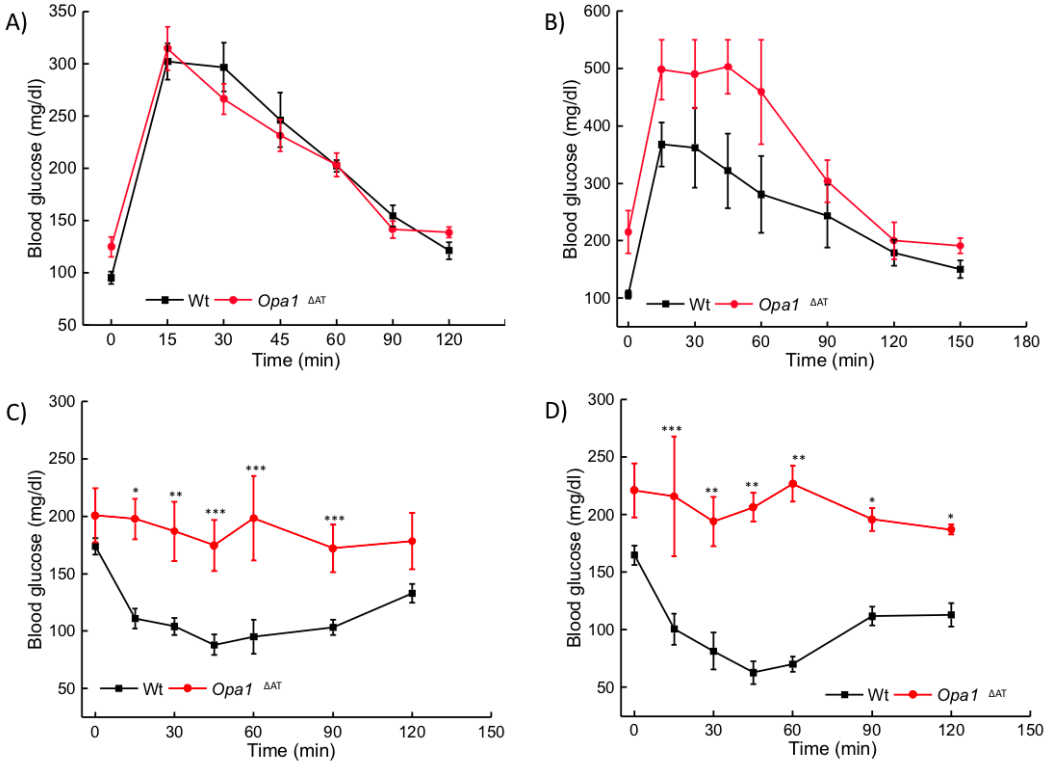

Figure 2. A), B) Average±SEM of blood glucose levels following an i.p. glucose tolerance test (GTT) performed on control and Opa1$^{\Delta AT}$ mice at the age of 8 weeks old (A) and 12 weeks old (B), n>3.

*C), D) Average±SEM of blood glucose levels following an i.p. insulin tolerance test (ITT) performed on control and Opa1$^{\Delta AT}$ mice at the age of 8 weeks old (C) and 12 weeks old (D), n>3. ***, p < 0.001; **, p < 0.01; *, p < 0.05 in a two-tailed Ttest.*

Interestingly, 8 weeks old mice Opa1 $^{\Delta AT}$ display no significant differences in total body weight, nor in lean and fat mass compared to Wt mice (Figure 1.A).

Notably, with the aging of the animals a significant progressive loss of fat mass was observed in Opa1 $^{\Delta AT}$ mice. No difference in the total body weight is detectable for a compensatory effect between the fat mass loss and the lean mass gain in the KO model (Figure 1.B and 1.C). 8 weeks old mice show similar glucose tolerance compared to controls, however at the age 12 weeks old Opa $^{\Delta AT}$ mice were found more glucose intolerant compared to Wt control, although no statistica significance was detected. Interestingly, both 8 and 12 weeks old Opa1 ΔAT mice show a significant disruption in the insulin sensitivity, resulting to be significantly more insulin resistant if compared to the Wt control (Figure 2.C and 2.D). This metabolic alteration is typically associated also with lipodystrophic phenotype and might be due to the higher degree of chronic inflammation caused by macrophagic infiltration [25].

All together this characterization strongly suggests that at the age of 8 weeks old the lipoatrophy already started, but it is not so widely spread to affect the metabolic functions of the adipose tissue. However, lipoatrophy will progressively worsen with the aging of the animal, eventually disrupting the adipose ability to maintain the whole-body homeostasis.

Because this process starts so early in the life of the mice, we deduced a crucial role of OPA1 in the maintenance of the physiologic state of the adipose tissue in mice.

5.2 Mice Opa1 $^{\Delta AT}$ challenged with HFD are unable to expand the fat mass

As Adipose tissue (AT) can respond rapidly and dynamically to alterations in nutrient deprivation and excess through adipocytes hypertrophy and hyperplasia, we decided to challenge our model with 4 weeks of High Feed Diet (HFD) at the age of 4 months, to accelerate the adipose tissue responses and metabolism without causing an excessive stress to the organ, figure 4.

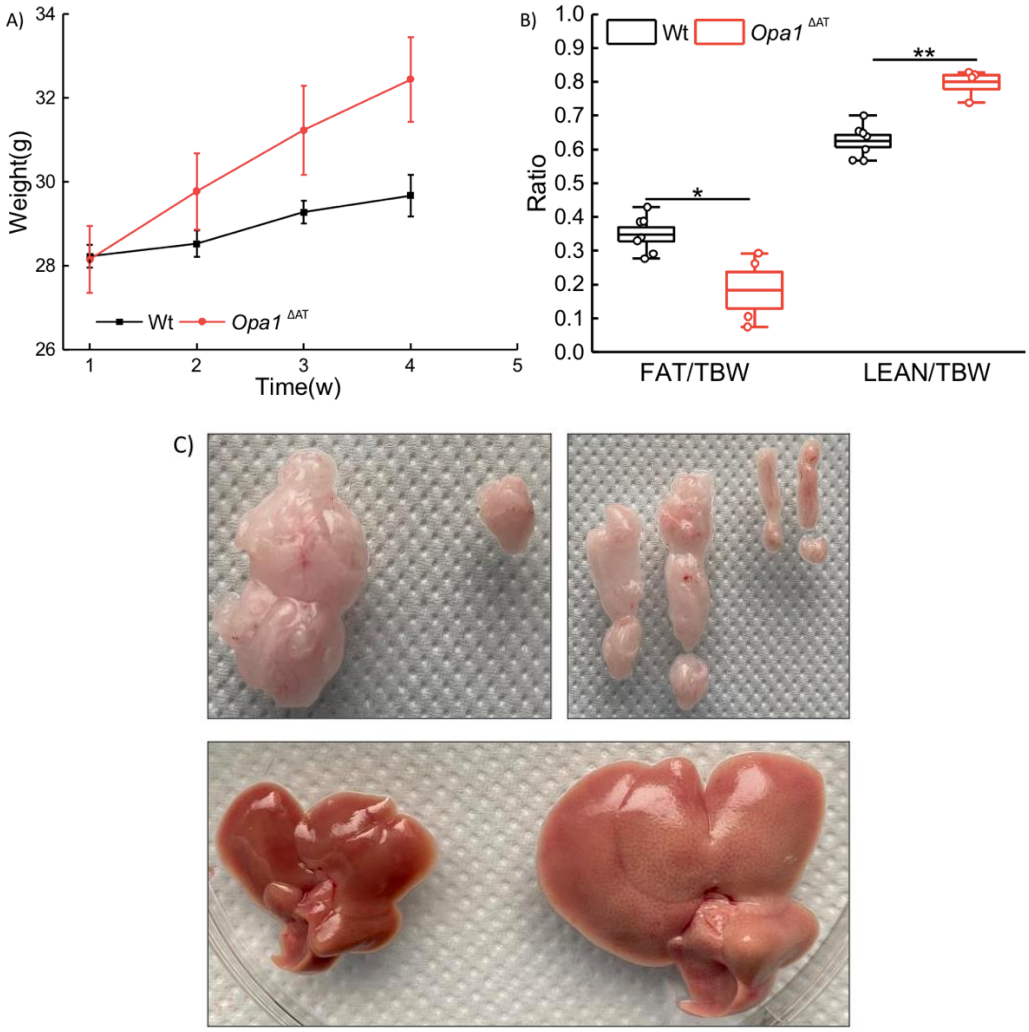

Figure 4. A) Average±SEM of total weight gain during 4 weeks of HFD, n>3 for each genotype. B) Boxplot of relative body composition assessed by EchoMRI, after 4 weeks of HFD, n>3 for each genotype. C) Representative images of, respectively, visceral and subcutaneous fat deports and liver of WT (right) and KO (left after 4 weeks of HFD.

Weight was recorded weekly and upon HFD Opa1$^{\Delta AT}$ mice gain less weight compared to Wt control (figure 4.a). Notably, observing the body composition after the challenge, we identify a statistical significance both in lean and fat mass between the KO and control (figure 4.B). This suggest that the OPA1 $^{\Delta AT}$ mice responded differently from the control, paradoxically gaining more lean mass and loosing fat tissue. Upon sacrifice of mice, we could appreciate the drastic reduction in the total volume of fat deposit in the OPA1 $^{\Delta AT}$, while the gain in lean mass corresponded to the enlargement of peripheral organs, such as heart and

liver, caused by ectopic fat deposition (figure 4.C). This could possibly indicate that the adipose tissue of Opa1 $^{\Delta AT}$ is unable to properly expand so to safely store the lipid excess, thus protecting the body from lipotoxic insult. Nevertheless, Hematoxylin and Eosin staining of paraffine-embedded subcutaneous fat deport highlighted the presence of big adipocytes in the Opa1 $^{\Delta AT}$ (black arrows), thus suggesting that the cells are indeed able to increase their size to accommodate more fat (Figure 5.A). Notably, a higher number of cell death events and fibrotic deposition (red arrows) are detectable in the Opa1 $^{\Delta AT}$. Dead adipocytes are easily recognizable as "crown like structure" (showed in figure 5.B), this distinguish structure is due to the macrophagic infiltration in the tissue to remove the dead cell [26].

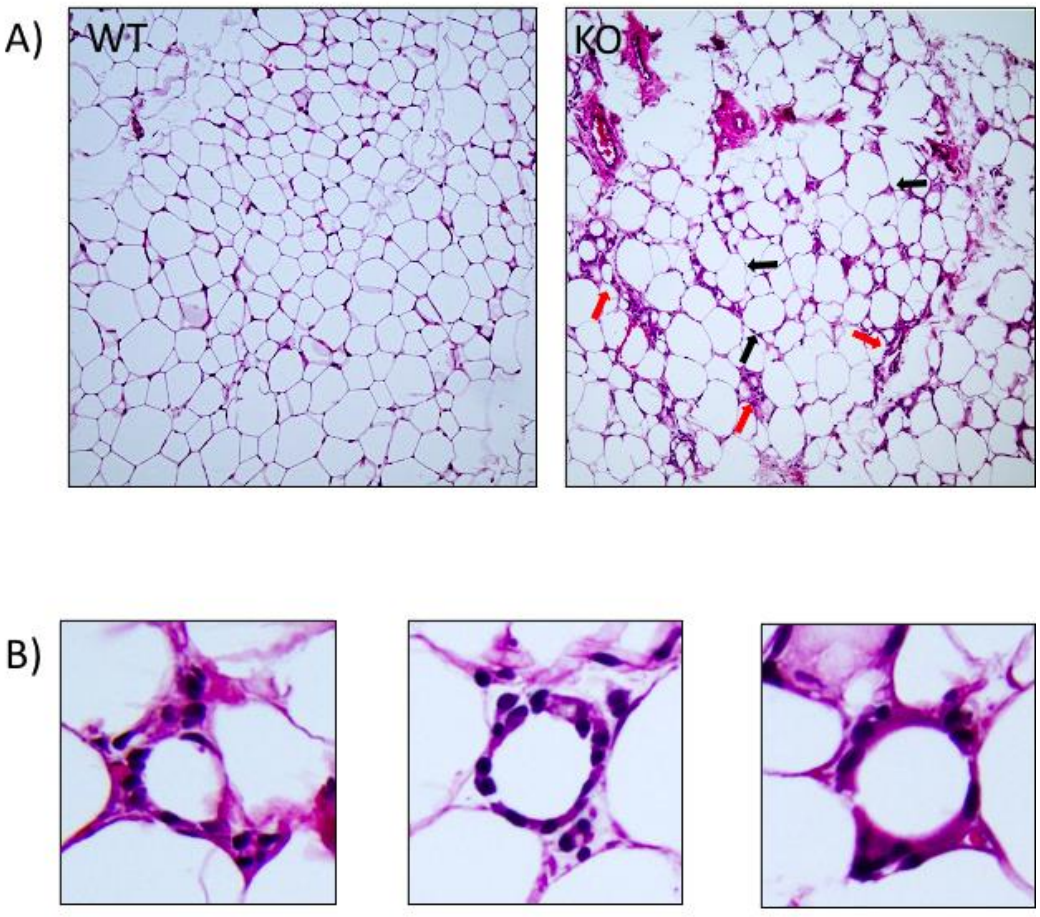

Figure 5. A) Representative Haematoxylin-Eosin stained sections of subcutaneous fat deport from 4 weeks old HFD WT and KO (images acquired with Leica LSM600, 10x). B) Representative magnification of a crown like structure.

The evident fibrotic deposition in the Opa1$^{\Delta AT}$ implies a pathological wound healing process in which the tissue is unable to restore the normal parenchyma, consequently substituted by scar tissue.

5.3 Impaired levels of PPARγ2 and disrupted OXPHOS in Opa1$^{\Delta AT}$

A crucial role in the maintenance of adipocytes physiology is covered by the peroxisome proliferator-activated receptor γ 2 (PPARγ2). Often referred as the master regulator of adipogenesis, in the last decades it was established its role in the survival of differentiated adipocytes. Indeed, PPARγ deletion in differentiated adipocytes resulted in cell death within few days from maturation, causing an overall progressive lipodystrophy [27], similarly to our model. Of note, mRNA expression level of PPARγ2 in whole subcutaneous tissue of Opa1$^{\Delta AT}$ was significant lower compared to the control (figure 6.C).

Recent studies have highlighted the relevance of ROS production and correct OXPHOS activity as a crucial feature in the metabolic homeostasis of the mature adipocytes [28]. Knowing the key role of OPA1 in the maintenance of the mitochondria structure and dynamics, we decided to evaluate both the respiratory chain integrity and two mitochondria shaping proteins, Mitofusin2 and DRP1, which play a key role in the events of fusion and fission, respectively. Results are shown in figure 6.A and 6.B.

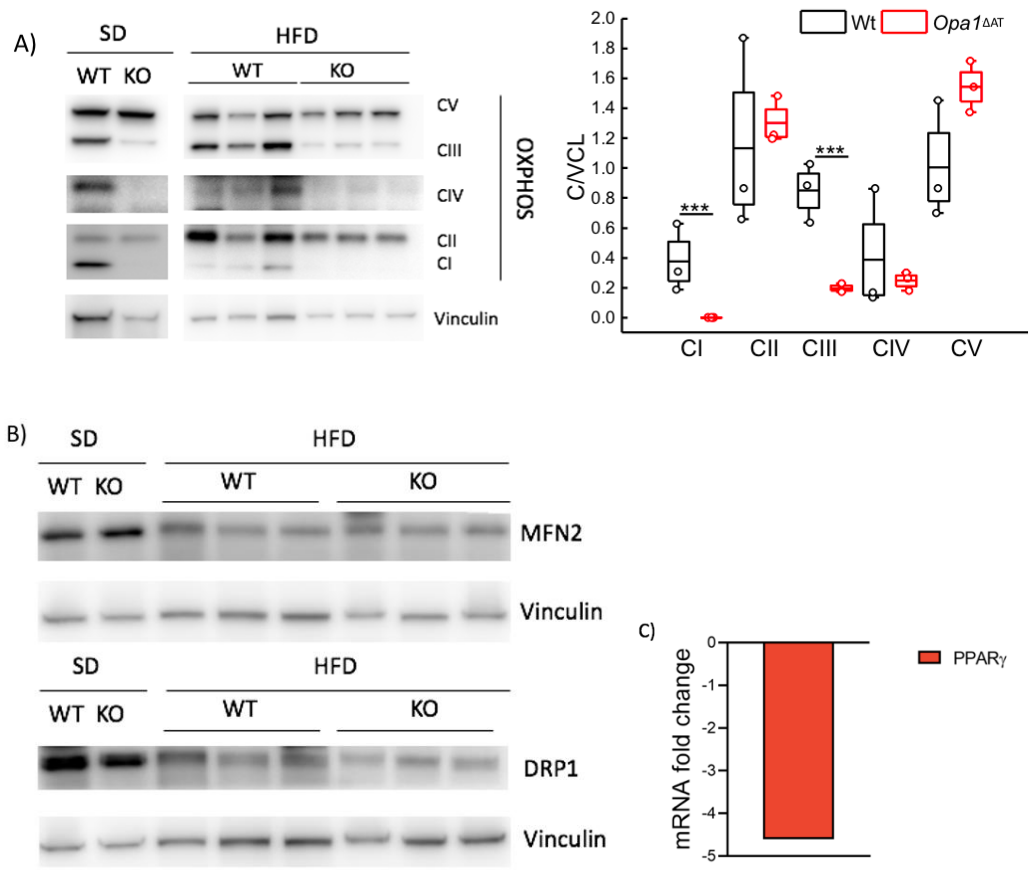

*Figure 6. A) Representative immunoblots using the indicated antibodies of equal amounts of protein (10 µg) from subcutaneous adipose tissue of WT and KO after 4 weeks HFD and control in Standard diet. N=3/genotype. Boxplot representing the relative quantification; ***, p< 0.001 in a two tailed Ttest B) Representative immunoblots using the indicated antibodies of equal amounts of protein (10 µg) from subcutaneous adipose tissue of WT and KO after 4 weeks HFD and control in Standard diet. C) mRNA expression level* of *PPARγ2. Data acquired with qRT-PCR from whole subcutaneous adipose tissue of KO and Wt mice. Analysis was performed with the* $2^{-\Delta\Delta C}$ *method. Data presented as fold reduction KO/WT (n=3/genotype).*

As expected, the mitochondrial respiratory chain is disrupted in the KO model, but to our surprise statistical analysis revealed a significant reduction specifically for complexes I and III (Figure 6.A). Notably, these two complexes of the electron-transport chain are the major sites for ROS production ([29]). Interestingly, no alteration was detected in the other mitochondrial shaping protein we evaluated (Figure 6.B). We could appreciate a tendency in the increase in MFN2 in the KO compared to the WT, nevertheless more animals should be analyzed.

5.4 YAP1 is downregulated in the adipose tissue of OPA1 KO mice

We sought to understand what could link different cellular processes, such as survival, expansion, reprogramming of metabolism and gene expression pattern and the mitochondria dysfunction in the adipose tissue. To narrow down the list of candidates we turned to RNA sequencing data published in Bean et al., unluckily there was no data provided for our KO model. Nevertheless, we decided to investigate the available data on the OPA^{tg} model, which display a generalized overexpression of the OPA1 protein. This model is particularly interesting because it is characterized by improved adipose tissue and metabolic function, smaller adipocytes and slightly resistance to HFD, as described in Bean et al., 2021. We identify, among all the less activated pathway, the Hippo pathway. This is a signaling pathway, well known in the cancer field, which exert a control over the activation and deactivation of its effectors YAP and TAZ, through a kinase signaling cascade. Briefly, as described in Figure 7, when Hippo pathway is switched off, YAP and TAZ are dephosphorylated and therefore can migrate in the nucleus, where they exert their function stabilizing the transcriptional factors TEAD. The effectors genes of this process are implicated in cell proliferation, survival, differentiation, morphology and migration as described in Heng et al., 2021.

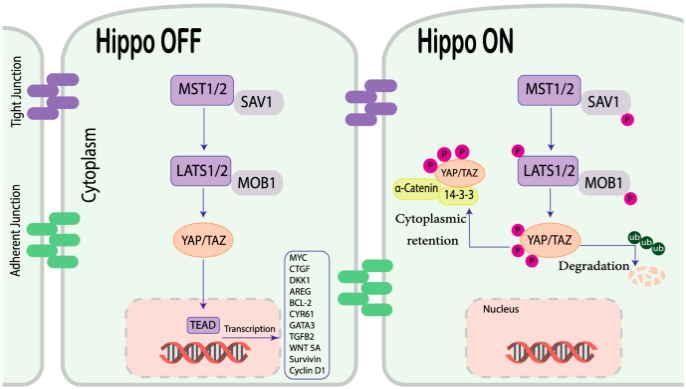

Figure 7. Hippo pathway regulation of YAP and TAZ, adapted from Heng et al., 2021

Additionally, Wang et al., 2020 demonstrated that the selective KO of YAP1 in the adipose tissue resulted in a lipodyatrophic phenotype which strongly correlate with the one displayed by our model. Nevertheless, the implications of the

YAP1/TAZ pathway in the adipose tissue still remains unclear under many aspects. Encouraged by the RNA sequencing data, we performed western blot analysis on whole subcutaneous tissue of HFD mice to evaluate the YAP1 pathway. Results are shown in Figure 8.

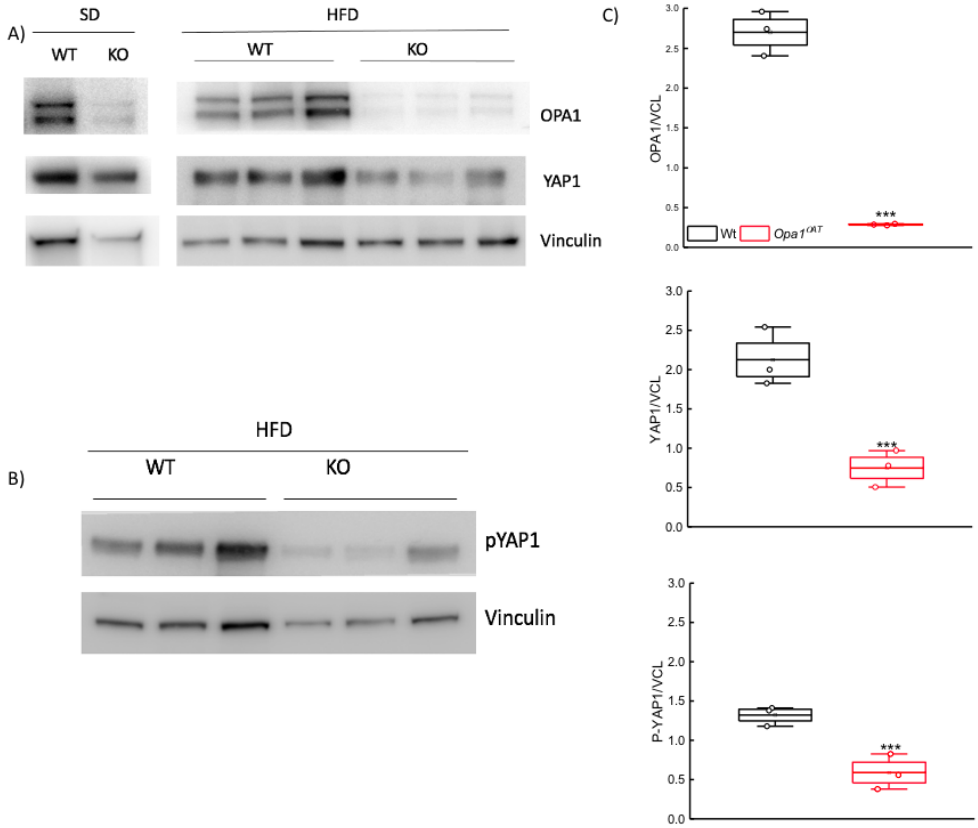

*Figure 8. A); B) Representative immunoblots using the indicated antibodies of equal amounts of protein (10 µg) from WT and Opa1 $^{\Delta AT}$ SAT after 4 weeks of HFD (n=3 independent experiments for each genotype). Vinculin was used as loading control. C) Quantification of OPA1, YAP1 and pYAP1 protein levels and ratio between pYAP/YAP in WT and KO (n=3; ***, p<0.001).*

Notably, we identified a significant reduction in the amount of total YAP1 in our KO model compared to the control, both in standard diet condition and HFD (Figure 8.A). We evaluated also the phosphorylated form of YAP1 (Figure 8.B) and interestingly also in this case we could see a reduction in the total amount of the protein. Because YAP1 is activated when dephosphorylated, we considered the

ratio between the two forms. Although no significant difference was observed, we could appreciate a tendency of increase in the KO compared to the WT, thus suggesting a possible deactivation of the pathway (Figure 8.C). a higher number of animals should be analyzed.

To further investigate the hypothesis of a downregulation of the YAP1 pathway in the OPA1 KO compared to WT, we evaluated the mRNA expression levels, in whole subcutaneous adipose tissue, of YAP1 main target genes: connective tissue growth factor (CTGF) and Cysteine-rich angiogenic inducer 61 (CYR61). We analyzed also the expression of the main inhibitors involved in the Hippo pathway: Angiomotin Like 2 (AMOTL2), Large Tumor Suppressor Kinase 1 and 2 (LATS1, LATS2) (Figure 9).

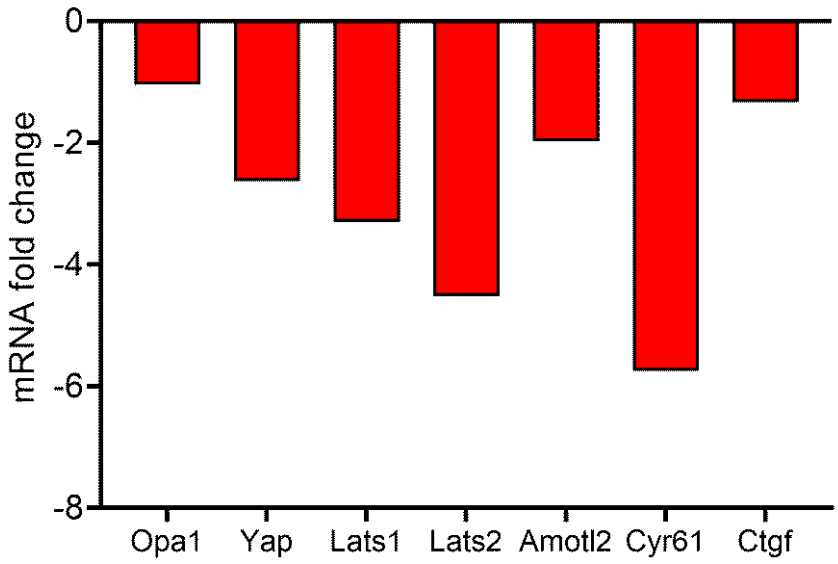

Figure 9. mRNA relative expression of YAP1 target genes and main inhibitors. Data acquired with qRT-PCR from whole subcutaneous adipose tissue of KO and Wt mice. Analysis was performed with the $2^{-\Delta\Delta C}$ method. Data presented as fold reduction KO/WT (n=3/genotype). Data normalized on actin.

Notably, the main target genes of YAP1 are highly downregulated when compared with WT, thus suggesting an inhibition of the pathway.

5.5 YAP1 localization in the adipose tissue

YAP1 is a coregulator factor which translocate to the nucleus to exert its function as both coactivator and corepressor of gene transcription. This means, that an efficient way to evaluate YAP1 activity is by localizing it in the cell. We therefore decided to perform immunofluorescence staining of paraffin-embedded SAT sections to understand if the higher amount of YAP1 in the control ultimately correlated to an activation of the pathway. Results show in Figure 10.

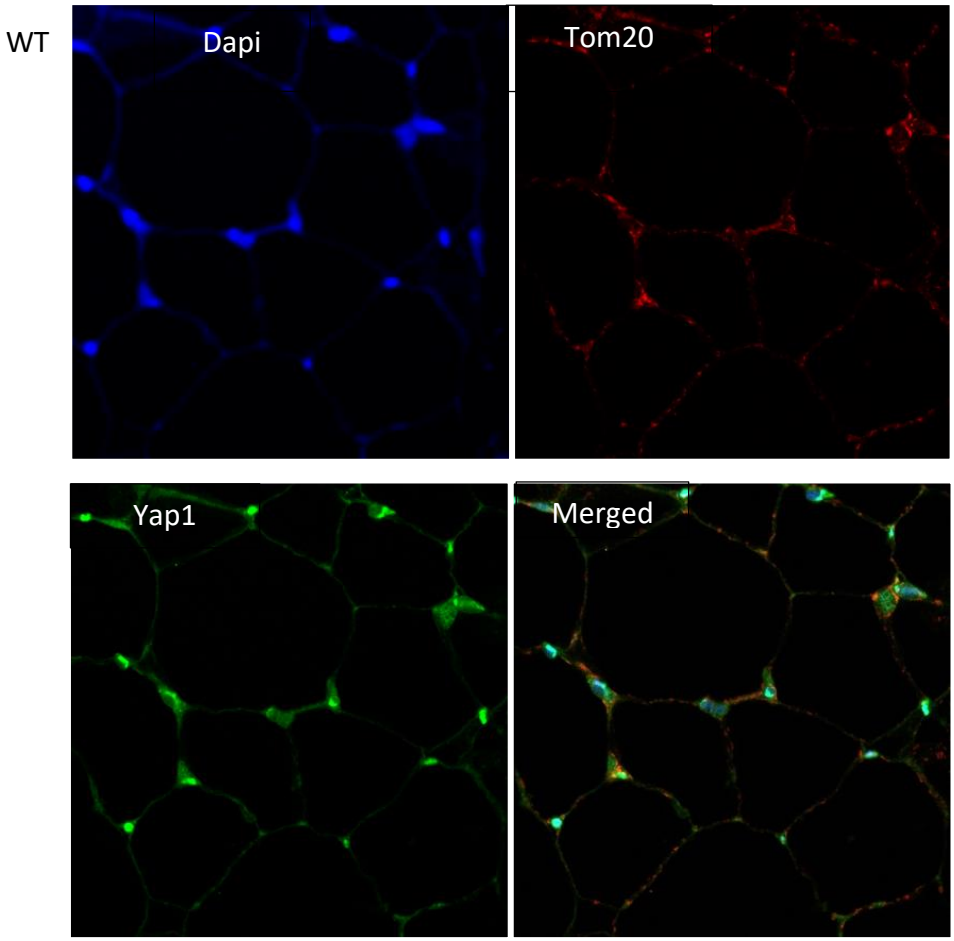

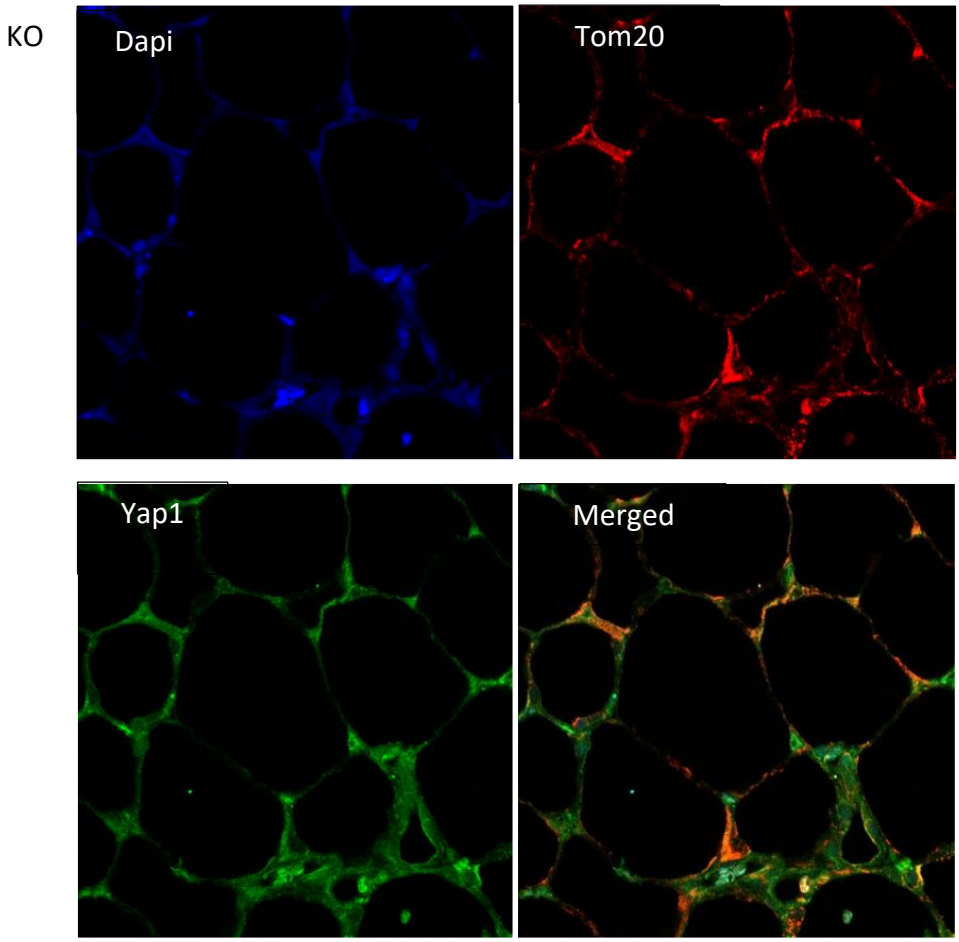

Figure 10. Immunofluorescence of paraffine-embended subcoutaneous adipose tissue of WT and KO mice, after 4 weeks of HFD. In Blu the nuclear staininer DAPI, in red mitochondrial marker TOM20, finally in green YAP1.

By keeping a qualitative approach, we might appreciate a higher colocalization of YAP1 (green) and the nuclei in the WT control (Figure 10) if compared with the KO. This is consistent with what already described in literature regarding YAP1 activation during HFD treatment [20]. Nevertheless, a more biochemical approach should be carried out and a higher number of animals should be analyzed.

Strikingly, we identified several areas which strongly indicates a colocalization of YAP1 and the mitochondrial marker TOM20, thus suggesting a possible interaction of YAP1 and the mitochondria (Figure 11). We therefore decided to perform a fractionation of fresh subcutaneous adipose tissue for each genotype to obtain

crude mitochondria pellet. We then evaluated the hypothesis by western blot analysis, results showed in Figure 11.

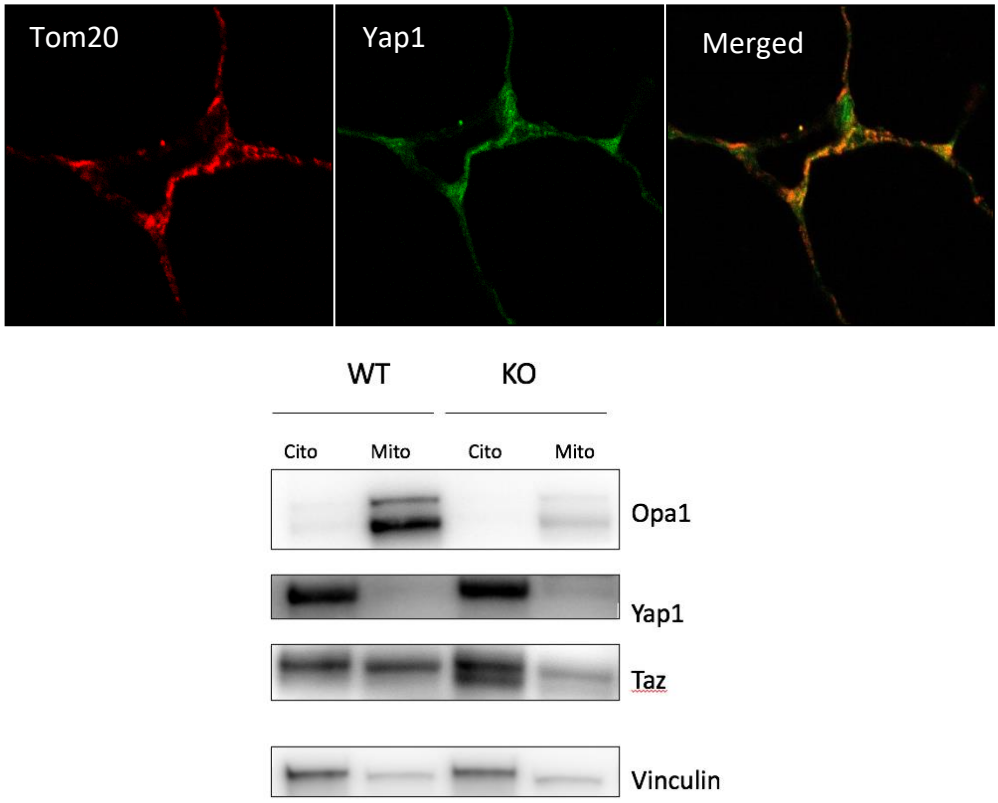

Figure 11. A) Representative images suggesting the colocalization of YAP1 and TOM20. B) Western blot analysis of the cytosolic and mitochondria fraction SAT of WT and KO mice in SD, aged 5 months.

Interestingly, we detect a small amount of YAP1 in the mitochondria fraction of Opa1$^{\Delta AT}$, but it could be correlated with the small cytosolic contamination which is evident by the presence of vinculin. To our surprise a more consistent amount of YAP1 paralog transcriptional co-activator with PDZ-binding motif (TAZ) is detectable in the mitochondrial fraction of both genotypes (Figure 11).
However, this preliminary evidence needs to be further studied.

5.6 Yap1 is downregulate during in vitro adipogenesis of cre-induced Opa1$^{\Delta AT}$ primary cells

We questioned if the downregulation of Yap1 in the Opa1$^{\Delta AT}$ model was directly depended on the loss of Opa1. So we decided to turn to an in vitro cell autonomous model: primary cells were extracted from the subcutaneous adipose tissue of WT mice (Opa1$^{flox/floxAT}$, n=9) after 4 weeks of HFD. Cells of the stromal vascular fraction, containing preadipocytes, were isolated and plated at a desired concentration and right after infected with Adeno-CRE virus, to induce the KO, or with GFP-virus as transfection control. After 24 hours from seeding, preadipocytes were induced into differentiation using adipogenic medium supplemented with insulin, IBMX, T3, rosiglitazone and dexamethasone differentiation (T0). After three days rosi and IBMX were removed (T3). The commitment toward the adipocyte lineage can be easily demonstrated by the distinctive morphology of adipocytes that store energy in the form of triglyceride-filled lipid droplets in the cytoplasm. Lipid droplets are detectable as early as 3 days post differentiation but reach full maturation at the stage of 6 days (Figure 12.A).

Protein lysate and RNA were collected before the induction (T0), at T3 and at full differentiation (T6), figure 12.

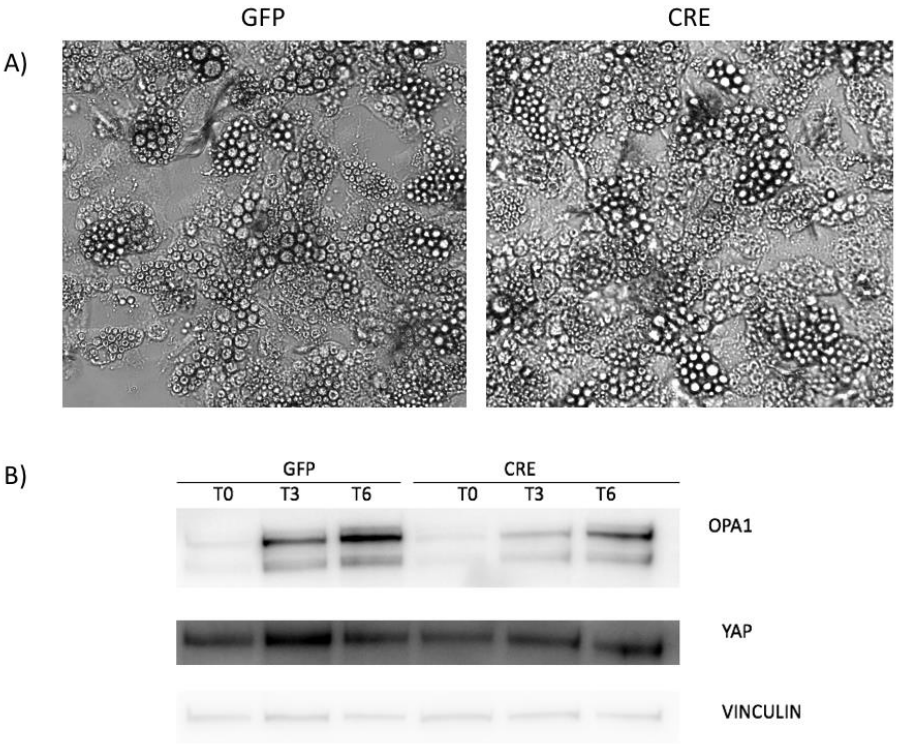
A)
GFP
CRE
B)
GFP
CRE
T0
T3
T6
T0
T3
T6
OPA1
YAP
VINCULIN
C)
mRNA fold change
800
600
400
200
0
T3 gfp
T3 cre
T6 gfp
T6 cre
T3 gfp
T3 cre
T6 gfp
T6 cre

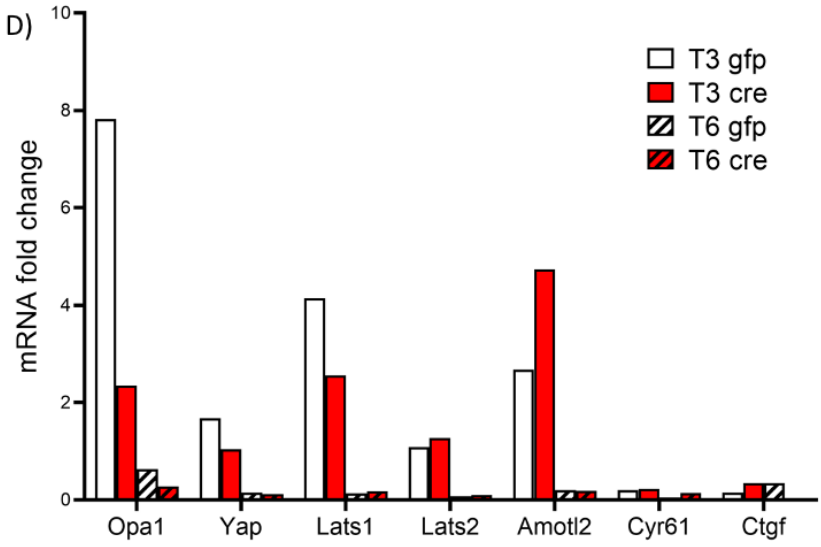

Figure 12. A) Representative Bright field images of cells OPA$^{f/f}$ in culture after transfection with adenoCre or GFP, stage of full differentiation (T6). B) Representative immunoblots using the indicated antibodies of equal amounts of protein (5 µg). Nine mice cOpa$^{f/f}$ were pooled together, cells were plated equally and transfected with either GFP as control of AdenoCRE to induce the KO of OPA1. Adipogenic differentiation was induced supplementing cells with appropriate media, samples were collecting at T0, T3 at full differentiation T6. Data represented as expression fold change T0 vs T3 and T0 vs T6.
C) mRNA relative expression of PPARγ and D) YAP1 target genes and main inhibitors. Data acquired with qRT-PCR from RNA collected from whole cell lysate. Analysis was performed with the $2^{-\Delta\Delta C}$ method. Data presented as fold reduction T0/T3 and T0/T6 for each condition. Data normalized on Pref1.

Western blot analysis and qRT-PCR confirm the successful outcome of the transfection, since levels of OPA1 in the Adeno-CRE infected cells are significantly lower both in the mRNA and protein expression. Interestingly, we identify a decreasing trend in the amount of YAP1 during adipogenesis of control cells: the reduction is more consistent in the first days of commitment and appears to be lighter in the maturation. This is consistent with what is already observed in literature, since the inactivation of the YAP/TAZ pathway is crucial for adipocytes commitment [19]. Looking at the induced KO cells, we noticed that this trend is inverted, with YAP1 increasing its amount in the latest

stages of differentiation, while a significant reduction occurs at the stage 3 (figure 12.B). Interestingly, this corresponds also to a solid reduction in the PPARγ2 mRNA expression level (figure 12.C). Notably, mRNA expression levels of YAP1 target genes (Figure 12.C) do not show a clear reduction in the OPA1 induced KO, thus further extending the complexity of the model. A compensatory mechanism orchestrated by the YAP1 paralogue TAZ might be hypothesized. It is indeed wide accepted the overlapping functions of these two proteins and, notably, the modulation in the amount of one has already been reported to affect the other (Kamura et al., 2018).

6. DISCUSSION

White adipose tissue displays the unique plasticity to expand both in cell size (hyperthropy) and number (hyperplasia), adjusting its metabolism to the nutritional state of the subject. The impairment of this adaptability cause adipocytes' dysfunctional state, and often culminate with cell death [1]. When this process is widely spread, the subject experiences loss of fat mass, a condition named lipoatrophy [27]. The WAT plays several key roles in the whole-body homeostasis; therefore, its disruption is closely related to systemic low-grade inflammation and metabolic disorders[2].

The relevance of studying the molecular mechanism underlying lipoatrophy is hence a crucial step to develop possible treatment strategies for pathological conditions associated with alterations in the adipose tissue mass and function.

Preliminary data suggested that the optic atrophy protein 1 (OPA1) is a key regulator of adipocyte size. The general overexpression of this protein (OPA^{tg}) improved the adipose and metabolic function. Whereas, the adipose tissue selective KO ($OPA^{\Delta AT}$) of this protein resulted in a complete opposite phenotype, characterized by extensive lipoatrophy, impaired metabolic function and ectopic fat deposition. A significant fibrotic deposition associated with cell death events and bigger adipocytes was detected, as described in Bean et al., 2021. We further investigated the phenotype of the KO model though Body mass composition analysis and common metabolic assay (GTT and ITT). We established that the lipoatrophy is an early, spontaneous event in the life of the mouse and progressively worsen with the aging of the animal. Indeed, as early as 8 weeks male KO mice displayed insulin resistance, typically associated with low degree of chronic inflammation and adipose impairment (de Luca & Olefsky, 2008), and lower (but not significant, $p < 0.06$) fat mass compared to the control. After only one month, the model displayed significant loss of adipose tissue, completely impaired insulin sensitivity and the beginning of glucose intolerance, with the

basal blood sugar being higher (but not significant, p <0.06) than the control. We reasoned that this early phenotype could be caused by an impairment in the mature adipocytes' physiology and/or metabolism. Indeed, for how our model is constructed, the excision of OPA1 occurs selectively in the mature cells. To better understand this strong phenotypic modulation orchestrated by OPA1, we challenged our model with 4 weeks of HFD, just to imprint the cells and stimulate the metabolism and plastic remodeling of the adipose tissue without causing excessive stress to the organ. We recorded weekly the body gain and body fat composition was acquired at the moment of sacrifice. Strikingly, both the KO and the control gained weight with no statistical difference, thus suggesting that both models took a comparable caloric intake. Nevertheless, the whole-body composition brought out a significant difference in FAT and LEAN mass: OPA $^{\Delta AT}$ gained significantly less fat mass, at the expense of the lean mass which, surprisingly, increased strongly, compared with the WT control. Upon sacrifice, we observed a drastic reduction in the size of fat deports in the KO and systemic ectopic fat deposition with marked steatotic hepatomegaly, thus explaining the gain in lean mass. Hematoxylin and Eosin staining showed a high number of cell death events and solid macrophagic infiltration, thus suggesting a low degree of chronic inflammation in the KO which was not detected in the WT. Interestingly, we could appreciate a comparable distribution in the size of the adipocytes between the KO and the control, thus suggesting that the OPA $^{\Delta AT}$ adipocytes preserve a consistent ability to enhance their size. We questioned if there might be an impairment in the delicate balance between lipogenesis and lipolysis. To assess so, we evaluated the expression levels in SAT (4 weeks of HFD) of two main enzymes involved in these opposite pathways, respectively Acetyl-CoA carboxylase (ACC) and Adipose triglyceride lipase (ATGL). Notably, western blot analysis did not detect any difference in the total amount of ACC, while mRNA expression level of the key lipolytic enzyme ATGL were strongly downregulated in the OPA $^{\Delta AT}$ compared with the control. This could suggest an impairment in the metabolism of the mature KO adipocytes, in which an excessive propension to lipid storage, is not counterbalanced by lipolytic events (data not showed).

PPARγ2 is a key regulator of terminal fat cell differentiation, but also regulates many genes involved in lipid transport and metabolism, insulin signaling and mature adipocytes physiology. Strikingly, the KO of this gene in the mature adipose cell results in apoptotic death within few days, leading to a systemic lipoatrophy [27]. Notably, the mRNA expression level of this gene in the SAT of male KO mice (4 weeks if HFD) is strongly reduced compared to the WT. Supplementation via injection with Rosiglitazione, an enhancer of PPARγ activity, managed to rescue the phenotype (unpublished data, Camilla Bean).

Evidences in literature suggest that a dysfunctional mitochondrial oxidative phosphorylation pathway in adipocytes results in an alteration of the white adipose mature cell [28]. Thinking at OPA1 as one of the most relevant mitochondrial protein implicated both in the maintenance of the structure and in the dynamics of the mitochondria, we decided to evaluate the OXPHOS and other mitochondrial shaping protein implicated in the process of fusion and fission. Western blot analysis of OXPHOS identified, as expected, a disruption in the mitochondria respiratory chain in $OPA^{\Delta AT}$ mice compared to control. Strikingly, the only most affected complexes are the III and I, these represent the main sources of ROS, which at lower-level acts second messengers also in the adipocytes [29]. Interestingly, it has been reported that an alteration in the OXPHOS chain results in metabolic alteration of the adipocytes (Masschelin et al., 2020). In the future it would be interesting to assess if the disruption of the OXPHOS actually correlates with a condition of oxidative stress, and if so, to establish the contribution of this process to the lipoatrophic phenotype displayed in the $OPA^{\Delta AT}$ mice. Notably, we could not identify any difference in the mitochondrial shaping protein Mitofusin 2 and Drp1. Nevertheless, more animals should be tested.

We decided to move forward, to sought for a possible pathway linking OPA1 and different cellular processes, such as survival, metabolic alteration and size regulation in the adipose tissue. We turned to the available RNA sequencing data of the OPA^{tg} model to identify a possible candidate. Among the most downregulated in the TG model, we identified the HIPPO pathway, which captured our attention: when switched off (as it appears in the OPA^{tg}) this kinase signaling

cascade ultimately ends with the activation of YAP and TAZ, two paralogue coregulators of gene expression positively implicated in cell proliferation, expansion, survival and in the regulation of the organ size. The implications of this pathway in the adipose tissue have already been reported, but still remains poorly characterized and contradictory for some aspects. We were encouraged by evidences in literature suggesting that KO of YAP1 and TAZ in HFD mice results in an overlapping lipodystrophy phenotype to the OPA$^{\Delta AT}$, characterized by high number of cells death events and strong macrophagic infiltration [20].

By combining western blot analysis and qRT-PCR we identified a significant reduction, compared to WT controls, in the total amount of YAP1 in OPA $^{\Delta AT}$ subcutaneous fat deposit of mice challenged with HFD for 4 weeks. We analyzed the mRNA expression levels of YAP1 main targets genes in the whole tissue and notably, we found a significant downregulation of the whole pathway. We decided to perform immunofluorescence staining of paraffine-embedded section of subcutaneous fat deport to localized YAP1 in the tissue. Indeed, because YAP1 is a transcriptional factor which translocate in the nucleus when activated through dephosphorylation, its localization in the cell is a golden standard to determine whether it is activated or not[16]. Consistently with what reported in the literature we identify a higher colocalization of YAP1 and the nuclear staining DAPI in the HFD control, thus suggesting a possible activation of the pathway[20]. Strikingly, we did not identify the same frequency of colocalization in the HFD KO model, thus possibly indicating an inactivation of the pathway. Nevertheless, a more biochemical approach should be carried out, for instance a nuclear/cytoplasmic fractionation followed by western blot analysis would be a good perspective.

Notably, we observed also a frequent colocalization of YAP1 signal and the mitochondria marker TOM20 in both genotypes, but with a higher occurrence in the KO model. Even though little to nothing is characterized in the literature about this possibility and we could not detect any predicted site of interaction using bioinformation tools, we decided to perform a crude mitochondria extraction from whole subcutaneous tissue of mice in SD. Through western blot analysis we could identify a timid band of YAP1 in the mitochondria fraction of OPA$^{\Delta AT}$ model

(undetected in the WT control) which anyway could be traced back to the cytoplasmic contamination. Nevertheless, we found a significant amount of the YAP1 paralog, TAZ both in the cytoplasmic fraction and in the mitochondrial fraction thus suggesting a possible localization of this protein in mitochondria. This preliminary observation opens intriguing perspective for the future, and will need further investigation to, first of all, confirm the actual localization of YAP1 and/or TAZ to the mitochondria.

Because the adipose tissue is a complex organ mainly, but not only, composed by adipocytes, we decided to turn to an in vitro cell autonomous model. To evaluate if the modulation of YAP1 was dependent on the lack of OPA1, we extracted primary cells from cOp1 flox/flox mice after 4 weeks of HFD and induced the deletion of Opa1 via AdenoCRE transduction. Cells were induced into differentiation with an adipogenic media protein lysates and RNA were collected at the given time point of differentiation (T0, T3, T6). By performing a western blot analysis, we confirmed the efficiency of the transfection and identified a reduction in the total amount of YAP1 specifically in the T3. This is a key moment in the differentiated cell, which follows the commitment and mark the beginning of the expression of adipogenic genes. Strikingly, the levels of PPARγ2 were significantly reduced at T3 and T6. It would be interesting to expand the timeline, so to define YAP1 modulation during the maturation of the adipose cell.

Looking at the expression levels of target genes of YAP1 we noticed a higher amount in the CRE treated cells, which is in discordance with our preliminary observations. Nevertheless, we suppose a compensatory mechanism carried out by TAZ, indeed it has been already observed how the modulation of one paralog affects the other: Kamura et al., 2018 demonstrated how the overexpression of YAP1 in the adipose tissue correlated with the downregulation of TAZ, which is indeed known to exert a negative effect on adipogenesis and PPARγ activity [18].

Further studies will be carried out to evaluate the hypothesis of a OPA1 dependent modulation of YAP1 expression and the possible compensatory mechanism carried out by its paralog TAZ.

7. RIASSUNTO

Con questo progetto di tesi abbiamo voluto investigare la possibile interazione tra la proteina mitocondriale OPA1 e il fattore di trascrizione YAP1 nel mantenimento della plasticità e adattabilità del tessuto adiposo bianco nel modello lipodistrofico $OPA1^{\Delta AT}$.

Questo organo è specializzato nella sintesi, accumulo e rilascio dei grassi. Grazie alla sua plasticità e adattabilità contribuisce al mantenimento dell'omeostasi del corpo. Quando l'espansione dell'adipocita è impedita o alterata, questo non riesce più ad esercitare il suo ruolo protettivo. Recentemente è stato scoperto che la proteina OPA1, un regolatore delle dinamiche mitocondriali, è in grado di regolare la capacità di espansione dell'adipocita. La sovra-espressione di OPA1 ($OPA1^{tg}$) nel tessuto adiposo ne aumenta la capacità di espansione, mentre il knock-out causa una forte lipoatrofia, che causa una lipotossicità a livello sistemico e l'insorgenza di alterazioni metaboliche, quali insulino resistenza e glucosio intolleranza.

Dati di sequenziamento suggeriscono che in questo processo sia coinvolto l'Hippo pathway e il suo effettore YAP1. Questo è uno dei più famosi regolatori delle dimensioni cellulari e svolge un ruolo chiave in molti altri processi che regolano la fisiologia di un tessuto, quali la proliferazione, il differenziamento e il destino cellulare in senso pro-apoptotico e di sopravvivenza. È stato inoltre riportato come YAP1 sia un modulatore del metabolismo cellulare, attraverso la regolazione delle dinamiche mitochondriali.

Il ruolo di questo pathway nell'adipocita rimane, tuttavia, ancora poco definito, molti dati contrastanti suggeriscono sia un effetto positivo che negativo sulla cellula adiposa. Recentemente, tuttavia, è emerso che l'attivazione di YAP1 e del suo paralogo TAZ negli adipociti maturi di animali sottoposti ad HFD è fondamentale per la sopravvivenza della cellula. Il doppio KO di questi fattori comporta lipodistrofia diffusa.

Abbiamo eseguito una caratterizzazione preliminare del nostro modello: i risultati ci suggeriscono che l'insorgenza della lipoatrofia è molto precoce (attorno ai due

mesi) e ha un andamento progressivo fino ai 6 mesi, momento in cui l'animale ha completamente perso tutti i depositi adiposi.

Il tessuto adiposo risponde ad un eccesso calorico aumentando il proprio metabolismo e dimensione attraverso i processi di iperplasia e ipertrofia, abbiamo sfruttato questa caratteristica per accorciare la finestra temporale della lipoatrofia. Dopo 4 settimane in HFD gli animali esibivano una marcata riduzione dei depositi adiposi rispetto ai controlli, accompagnata da forte lipotossicità periferica. Sezioni istologiche con colorazione ad ematossilina ed eosina identificano la presenza di adipociti di grandi dimensioni, accostati però da molti eventi di morte cellulare. Questo ci ha comunque suggerito una buona capacità ipertrofica dell'adipocita $OPA^{\Delta AT}$. Dati di pRT-PCR rilevano livelli molto bassi di PPARy2 nel topo KO rispetto al controllo WT. È interessante notare che in letteratura vi è descritto un fenotipo lipoatrofico sovrapponibile al nostro causato dal KO di PPARy2 nell'adipocita maturo.

L'analisi mediate western blot e qRT-PCR una riduzione del livello di YAP1 e dei suoi effettori in seguito al *knock out* di OPA1 rispetto al controllo WT. Questo potrebbe suggerire un'inattivazione del pathway. Abbiamo eseguito delle immunofluorescenze su tessuto per identificare la localizzazione nella cellula di questo fattore di trascrizione, bisogna infatti considerare che l'attivazione di YAP1 è direttamente correlata con la sua traslocazione nel nucleo. Mantenendo un approccio qualitativo abbiamo potuto apprezzare una più precisa localizzazione nucleare di YAP1 nel controllo, che non è così evidente nel modello KO.

La nostra attenzione è stata catturata da un elevato numero di co-localizzazione di YAP1 e del marker mitocondriale Tom20. Nonostante analisi bioinformatiche su piattaforme come Deepmito, abbiano scartato la presenza di sequenze di riconoscimento mitocondriale su YAP1, abbiamo eseguito un frazionamento da tessuto sottocutaneo, ottenendo un pellet di mitocondri crudi. Analisi westernblot suggerirebbero la presenza nella frazione mitocondriale di una piccola frazione di YAP1 e di una più sostanziosa del paralogo TAZ.

Infine, per identificare se la variazione nella quantità totale di YAP1 che osserviamo nel modello KO è dipendente dal KO di OPA1, ci siamo spostanti su un

modello in vitro di colture primarie $OPA^{f/f}$. Il KO è stato indotto attraverso la trasfezione con AdenoCRE. Anche in questo caso abbiamo identificato una marcata riduzione di YAP1, soprattutto a T3, ma non dei suoi effettori. Questi dati potrebbero suggerire un coinvolgimento anche del paralogo di YAP1, TAZ poiché la sua attivazione è correlata con i medesimi geni target. È doveroso sottolineare che PPARγ è downregolato dall'attivazione di TAZ e che in letteratura è già stato identificato come la modulazione nella quantità di uno dei due paraloghi si ripercuote sull'altro.

8. REFERENCES

1. Choe, S. S., Huh, J. Y., Hwang, I. J., Kim, J. I. & Kim, J. B. Adipose tissue remodeling: Its role in energy metabolism and metabolic disorders. *Frontiers in Endocrinology* vol. 7 Preprint at https://doi.org/10.3389/fendo.2016.00030 (2016).
2. Luo, L. & Liu, M. Adipose tissue in control of metabolism. *Journal of Endocrinology* vol. 231 R77–R99 Preprint at https://doi.org/10.1530/JOE-16-0211 (2016).
3. Pellegrinelli, V., Carobbio, S. & Vidal-Puig, A. Adipose tissue plasticity: how fat depots respond differently to pathophysiological cues. *Diabetologia* vol. 59 1075–1088 Preprint at https://doi.org/10.1007/s00125-016-3933-4 (2016).
4. Cannon, B. & Nedergaard, J. Brown Adipose Tissue: Function and Physiological Significance. (2004) doi:10.1152/physrev.00015.2003.-The.
5. Bean, C. *et al.* The mitochondrial protein Opa1 promotes adipocyte browning that is dependent on urea cycle metabolites. *Nature Metabolism* **3**, 1633–1647 (2021).
6. Mulya, A. & Kirwan, J. P. Brown and Beige Adipose Tissue: Therapy for Obesity and Its Comorbidities? *Endocrinology and Metabolism Clinics of North America* vol. 45 605–621 Preprint at https://doi.org/10.1016/j.ecl.2016.04.010 (2016).
7. Dai, W. & Jiang, L. Dysregulated Mitochondrial Dynamics and Metabolism in Obesity, Diabetes, and Cancer. *Frontiers in Endocrinology* vol. 10 Preprint at https://doi.org/10.3389/fendo.2019.00570 (2019).
8. Haczeyni, F., Bell-Anderson, K. S. & Farrell, G. C. Causes and mechanisms of adipocyte enlargement and adipose expansion. *Obesity Reviews* vol. 19 406–420 Preprint at https://doi.org/10.1111/obr.12646 (2018).
9. Eckel-Mahan, K., Ribas Latre, A. & Kolonin, M. G. Adipose Stromal Cell Expansion and Exhaustion: Mechanisms and Consequences. *Cells* vol. 9 Preprint at https://doi.org/10.3390/cells9040863 (2020).
10. Lindhorst, A. *et al.* Adipocyte death triggers a pro-inflammatory response and induces metabolic activation of resident macrophages. *Cell Death and Disease* **12**, (2021).
11. Zatterale, F. *et al.* Chronic Adipose Tissue Inflammation Linking Obesity to Insulin Resistance and Type 2 Diabetes. *Frontiers in Physiology* vol. 10 Preprint at https://doi.org/10.3389/fphys.2019.01607 (2020).
12. Wang, F., Mullican, S. E., DiSpirito, J. R., Peed, L. C. & Lazar, M. A. Lipoatrophy and severe metabolic disturbance in mice with fat-specific deletion of PPARγ. *Proc Natl Acad Sci U S A* **110**, 18656–18661 (2013).
13. de Pauw, A., Tejerina, S., Raes, M., Keijer, J. & Arnould, T. Mitochondrial (dys)function in adipocyte (de)differentiation and systemic metabolic alterations. *American Journal of Pathology* vol. 175 927–939 Preprint at https://doi.org/10.2353/ajpath.2009.081155 (2009).

14. Noguchi, M. & Kasahara, A. Mitochondrial dynamics coordinate cell differentiation. *Biochemical and Biophysical Research Communications* **500**, 59–64 (2018).
15. Cogliati, S., Enriquez, J. A. & Scorrano, L. Mitochondrial Cristae: Where Beauty Meets Functionality. *Trends in Biochemical Sciences* vol. 41 261–273 Preprint at https://doi.org/10.1016/j.tibs.2016.01.001 (2016).
16. Piccolo, S., Dupont, S. & Cordenonsi, M. The biology of YAP/TAZ: Hippo signaling and beyond. *Physiological Reviews* **94**, 1287–1312 (2014).
17. Totaro, A., Panciera, T. & Piccolo, S. YAP/TAZ upstream signals and downstream responses. *Nature Cell Biology* vol. 20 888–899 Preprint at https://doi.org/10.1038/s41556-018-0142-z (2018).
18. el Ouarrat, D. *et al.* TAZ Is a Negative Regulator of PPARγ Activity in Adipocytes and TAZ Deletion Improves Insulin Sensitivity and Glucose Tolerance. *Cell Metabolism* **31**, 162-173.e5 (2020).
19. Lorthongpanich, C. *et al.* YAP as a key regulator of adipo-osteogenic differentiation in human MSCs. *Stem Cell Research and Therapy* **10**, (2019).
20. Wang, L. *et al.* YAP and TAZ protect against white adipocyte cell death during obesity. *Nature Communications* **11**, (2020).
21. Patten, D. A. *et al.* OPA1-dependent cristae modulation is essential for cellular adaptation to metabolic demand. *The EMBO Journal* **33**, 2676–2691 (2014).
22. Huang, S. *et al.* Yap regulates mitochondrial structural remodeling during myoblast differentiation. *American Journal of Physiology - Cell Physiology* **315**, C474–C484 (2018).
23. Bruder, J. & Fromme, T. Global Adipose Tissue Remodeling During the First Month of Postnatal Life in Mice. *Frontiers in Endocrinology* vol. 13 Preprint at https://doi.org/10.3389/fendo.2022.849877 (2022).
24. Kodde, A. *et al.* Maturation of White Adipose Tissue Function in C57BL/6j Mice From Weaning to Young Adulthood. *Frontiers in Physiology* **10**, (2019).
25. de Luca, C. & Olefsky, J. M. Inflammation and insulin resistance. *FEBS Letters* vol. 582 97–105 Preprint at https://doi.org/10.1016/j.febslet.2007.11.057 (2008).
26. Murano, I. *et al.* Dead adipocytes, detected as crown-like structures, are prevalent in visceral fat depots of genetically obese mice. *Journal of Lipid Research* **49**, 1562–1568 (2008).
27. Imai, T. *et al. Peroxisome proliferator-activated receptor is required in mature white and brown adipocytes for their survival in the mouse*. www.pnas.orgcgidoi10.1073pnas.0400356101 (2004).
28. Schöttl, T., Kappler, L., Fromme, T. & Klingenspor, M. Limited OXPHOS capacity in white adipocytes is a hallmark of obesity in laboratory mice irrespective of the glucose tolerance status. *Molecular Metabolism* **4**, 631–642 (2015).
29. Tormos, K. v. *et al.* Mitochondrial complex III ROS regulate adipocyte differentiation. *Cell Metabolism* **14**, 537–544 (2011).

30. Heng, B. C. *et al.* An overview of signaling pathways regulating YAP/TAZ activity. *Cellular and Molecular Life Sciences* vol. 78 497–512 Preprint at https://doi.org/10.1007/s00018-020-03579-8 (2021).
31. Kamura, K. *et al.* Obesity in Yap transgenic mice is associated with TAZ downregulation. *Biochemical and Biophysical Research Communications* **505**, 951–957 (2018).
32. Masschelin, P. M., Cox, A. R., Chernis, N. & Hartig, S. M. The Impact of Oxidative Stress on Adipose Tissue Energy Balance. *Frontiers in Physiology* vol. 10 Preprint at https://doi.org/10.3389/fphys.2019.01638 (2020).